*Published online 12 April 2013*

*Nucleic Acids Research, 2013, Vol. 41, No. 11* ***e115***
*doi:10.1093/nar/gkt255*

# Development of an assay to measure mutagenic non-homologous end-joining repair activity in mammalian cells

**Ranjit S. Bindra[1], Alexander G. Goglia[1], Maria Jasin[2] and Simon N. Powell[1,3,*]**

[1]Department of Radiation Oncology, Memorial Sloan-Kettering Cancer Center (MSKCC), New York, NY 10065, USA, [2]Developmental Biology Program, MSKCC, New York, NY 10065, USA and [3]Molecular Biology Program, MSKCC, New York, NY 10065, USA

Received December 19, 2012; Revised March 15, 2013; Accepted March 19, 2013

## ABSTRACT

**Double-strand break (DSB) repair pathways are critical for the maintenance of genomic integrity and the prevention of tumorigenesis in mammalian cells. Here, we present the development and validation of a novel assay to measure mutagenic non-homologous end-joining (NHEJ) repair in living cells, which is inversely related to canonical NHEJ and is based on the sequence-altering repair of a single site-specific DSB at an intrachromosomal locus. We have combined this mutagenic NHEJ assay with an established homologous recombination (HR) assay such that both pathways can be monitored simultaneously. In addition, we report the development of a ligand-responsive I-SceI protein, in which the timing and kinetics of DSB induction can be precisely controlled by regulating protein stability and cellular localization in cells. Using this system, we report that mutagenic NHEJ repair is suppressed in growth-arrested and serum-deprived cells, suggesting that end-joining activity in proliferating cells is more likely to be mutagenic. Collectively, the novel DSB repair assay and inducible I-SceI will be useful tools to further elucidate the complexities of NHEJ and HR repair.**

## INTRODUCTION

DNA double-strand breaks (DSBs) are among the most potentially lethal types of DNA damage in cells, as even a single unrepaired DSB can result in genetic instability and tumorigenesis (1). DSBs can arise from endogenous sources, such as replication and cellular endonucleases, and also from exogenous sources, such as ionizing radiation (IR) and many chemotherapy regimens (2). Accordingly, cells have evolved a number of DSB repair pathways to address these lesions. Non-homologous end-joining (NHEJ) and homologous recombination (HR) comprise the two major pathways by which DSBs are repaired in cells. NHEJ processes and re-ligates the exposed DNA termini of DSBs without the use of significant homology, whereas HR uses homologous DNA sequences as a template for repair (3). HR predominates in S-phase cells, when a sister chromatid is available as a template for repair, and is a high-fidelity process (4). NHEJ is thought to be active throughout the cell cycle, and it is more error-prone compared with HR. Another DSB repair pathway has been described, single-strand annealing (SSA), which anneals adjacent sequence repeats flanking a DSB, resulting in a deletion between the repeats (5).

Emerging evidence indicates that multiple sub-pathways exist by which DSBs are processed within both NHEJ and HR. In particular, it is now widely accepted that NHEJ repair comprises both canonical NHEJ (cNHEJ) and non-canonical pathways (6). The former pathway results in minimal processing of the DSB during repair, whereas the latter pathway typically results in larger insertions or deletions, with or without the use of sequence microhomology for re-ligation (7). Critical cNHEJ proteins include DNA-dependent protein kinase catalytic subunit (DNA-PKcs), the Ku70 and Ku80 heterodimer, X-ray cross-complementing-4 (XRCC4) and ligase IV [LigIV (8)]. Non-canonical NHEJ repair pathways and their corresponding proteins remain poorly defined, and multiple names have been assigned to them, including alternative NHEJ [aNHEJ or alt-NHEJ (9)], back-up NHEJ [bNHEJ (10)] and microhomology-mediated end-joining (11). For clarity, we will refer to these pathways collectively as either non-canonical or mutagenic NHEJ repair in this manuscript. Previous studies have suggested that several proteins play a role in these non-canonical pathways,

*To whom correspondence should be addressed. Tel: +212 639 6072; Fax: +212 794 3188; Email: Powells@mskcc.org
Present address:
Ranjit S. Bindra, Department of Therapeutic Radiology, Yale School of Medicine, New Haven, CT 06520, USA.

including ligase III (LigIII), ligase I (LigI), XRCC1 and poly(ADP-ribose) polymerase-1 [PARP-1(6)]. However, several recent reports have called into the question whether LigIII and XRCC1 are actually required for these alternative NHEJ pathways (12–15). In addition, Iliakis and colleagues (10,16–18) have reported the intriguing finding that non-canonical NHEJ (which they refer to as bNHEJ) is suppressed in growth-arrested and serum-deprived cells. Taken together, these findings highlight the complexities of NHEJ repair pathways, and they also suggest that further studies are needed to fully elucidate the sub-pathways and proteins involved in these processes.

A large number of assays have been developed to study both NHEJ and HR repair. Plasmid rejoining assays in transfected cells and protein extracts were used initially, and they have yielded enormous insights into DSB repair mechanisms (19). More recently, numerous assays with intrachromosomally based substrates have been developed to study NHEJ, HR and SSA repair in mammalian cells. The majority of these assays are fluorescence based and use the rare cutting endonuclease, I-SceI, to induce a single site-specific DSB in cells (20). The direct repeat green fluorescent protein (DR-GFP) assay is a commonly used assay to measure HR in living cells [schematic shown in Figure 2B (21)]. In this system, the 24-bp recognition site of I-SceI has been integrated into the *GFP* gene such that it disrupts the open reading frame (ORF) of the gene, and a truncated *GFP* gene fragment with the correct ORF sequence has been placed downstream in the construct. Repair of the cleaved I-SceI site by HR using the downstream fragment gives rise to a functional *GFP* gene, and GFP fluorescence then can be measured by flow cytometry. Similar GFP-based assays have been developed to measure both cNHEJ and non-canonical NHEJ in cells. Most of these systems are based on two adjacent I-SceI sites, without a downstream homology template. Simultaneous cleavage of both sites typically results in a 'pop-out' fragment which, depending on the orientation of the two I-SceI sites, creates either complementary or non-complementary overhangs that are exclusively repaired by NHEJ (22–25). Limitations of these current NHEJ assays include the need to induce two DSBs at a single locus, low frequencies of GFP+ cells after DSB induction, and conflicting results regarding the dependencies of various NHEJ proteins on repair activity (26,27). For example, publications have reported that Ku70/80 downregulation does not affect overall NHEJ repair frequencies using an assay based on two I-SceI sites (22), whereas other studies have suggested that loss of these proteins has a significant effect on repair rates in similarly designed NHEJ assays (24,28). Finally, DSB repair assays recently have been described in which mutagenic NHEJ repair of a nuclease-induced DSB causes loss of fluorescent protein expression via disruption of the ORF, or a specific insertion/deletion restores the ORF of a frame-shifted fluorescent protein (29–31). These findings suggest that additional assays to measure NHEJ repair are needed to further elucidate these sub-pathways and also the roles of individual DSB repair proteins.

Here, we present the development and validation of a novel intrachromosomal NHEJ assay based on the repair of a single site-specific DSB. In this system, the I-SceI site has been incorporated in-frame into the ORF of a repair substrate, such that any repair events that disrupt the ORF result in DsRed fluorescence from a separately integrated reporter vector. Thus, our assay is a reporter of mutagenic NHEJ repair. This assay can be rapidly integrated into cells at intrachromosomal loci, and it can be combined with HR assays as a means to measure key DSB repair pathways simultaneously in living cells. We also describe a novel, ligand-inducible I-SceI system for DSB induction, which was developed during the course of these studies. This system also can be stably integrated into cells, thus allowing precise control of cleavage kinetics without the requirement for I-SceI plasmid transfection. Surprisingly, incorporation of our NHEJ assay into several different cell lines indicates that mutagenic NHEJ repair is a robust process, yielding percentages of DsRed+ cells ranging from 20 to 60% after DSB induction. We also corroborate previous findings that cNHEJ suppresses mutagenic NHEJ repair (22,32,33) in a focused RNA interference (RNAi) screen, and that LigIII and XRCC1 may not be required for the latter repair pathway. In addition, we demonstrate that mutagenic NHEJ is suppressed in both growth-arrested and serum-deprived cells using our assay. This system will be an important tool for future studies focused on further elucidating NHEJ sub-pathways, and our novel inducible I-SceI will be useful for other applications in which better control of site-specific cleavage is needed.

## MATERIALS AND METHODS

### Plasmids

The two plasmids in our EJ-RFP system were derived from vectors included in the T-REx™ core kit, a commercially available tetracycline-regulated mammalian expression system (Invitrogen Corporation). The *TetR* ORF is encoded in pCDNA6/TR of the T-REx™ system, and it contains a unique in-frame XbaI site immediately downstream from the ATG start codon, which we used to clone in an I-SceI site. Specifically, the *TetR* ORF from pCDNA6/TR was amplified with a forward primer containing another XbaI site followed by an I-SceI site, and a reverse primer containing an XbaI site after the stop codon of the *TetR* ORF. Of note, the aforementioned unique XbaI site after the ATG start codon in the *TetR* ORF was intentionally destroyed in the forward primer by a silent single base pair substitution (thus, without modifying the amino acid sequence of the *TetR* ORF), which would allow subsequent downstream re-cloning using the newly introduced XbaI in the forward primer. This polymerase chain reaction (PCR) amplicon was then cloned back into the pCDNA6/TR vector at the aforementioned XbaI site after the ATG start codon. This plasmid was named Sce-TetR. To create the TO-DsRed reporter substrate, a *DsRed* gene ORF was amplified with KpnI and XbaI sites and cloned into the corresponding sites in the multiple cloning region of pCDNA4/TO of the T-REx™ system.

Our novel inducible I-SceI construct was derived from a previously described fusion gene construct consisting of a fusion between the I-SceI gene and the ligand-binding domain of the rat glucocorticoid receptor (GR) on the C-terminus and an RFP gene on the N-terminus (34). The I-SceI ORF and the C-terminal GR domain were amplified by PCR with primers containing an NheI site on the 5′-end and an XbaI site on the 3′-end. This amplicon was then cloned into a unique XbaI site in the multiple cloning region of pTuner-N, a commercially available plasmid that contains the Shield1 ligand-dependent destabilization domain (dd) as an N-terminal fusion driven by a cytomegalovirus (CMV) promoter (Clontech Laboratories, Inc.). The NheI and XbaI restriction enzymes create compatible cohesive ends, and cleavage at the latter site in pTuner-N requires passage of the plasmid in *dam*−/*dcm*− cells because of Dam/Dcm methylation. This new plasmid was named ddSceGR. For transient I-SceI plasmid transfections, we used the previously described expression vector, pCBASce (35).

### Cell lines and culture conditions

RKO colorectal and M059K glioma cell lines were obtained from the American Type Culture Collection (ATCC). U2OS-DR cells, which contain a chromosomally integrated DR-GFP assay to measure HR repair, have been described previously (36). RKO, U2OS-DR and derivative cell lines were cultured in high glucose Dulbecco's modified Eagle's medium (DMEM) with L-glutamine containing 10% tetracyline-free (tet-free) fetal bovine serum (FBS; Clontech Laboratories and Atlanta Biologics). M059K cells were cultured in DMEM/F12 media supplemented with 10% tet-free FBS (Invitrogen), 0.05 mM non-essential amino acids, 0.5 mM sodium pyruvate and 15 mM 4-(2-hydroxyethyl)-1-piperazineethanesulfonic acid. All cells were maintained at 37°C with 5% $CO_2$. Tet-free serum was required to prevent *DsRed* gene expression in the EJ-RFP system from residual tetracycline found in most commercially available FBS preparations. For studies involving ddSceGR, cells were cultured in charcoal-stripped FBS (Invitrogen Corporation) to minimize the levels of endogenous glucocorticoids present in untreated FBS preparations. For the experiments involving serum deprivation, cells were washed two times in DMEM containing reduced FBS concentrations to remove residual serum, followed by replacement of the culture medium with DMEM containing 0.1% FBS.

The EJ-RFP assay plasmids were stably integrated into RKO, M059K and U2OS-DR cells using a fluorescence-activated cell sorting (FACS) enrichment strategy, which is described in detail in the 'Results' section. Briefly, plasmid transfection was performed by nucleofection in these cell lines (Lonza corporation), and blasticidin and zeocin antibiotics were used to select for cells containing integrated copies of the Sce-TetR and TO-DsRed vectors, respectively, as per the manufacturer's specifications. At the indicated times, sterile doxycycline (Sigma-Aldrich Co., LLC) was added to cell cultures at a concentration of 1 μg/ml to induce de-repression of *DsRed* gene expression. Cells were subjected to sterile FACS-based enrichment using standard protocols at the MSKCC Flow Cytometry Core Facility. When indicated, single cell clones were isolated by limiting dilution in 96-well microplates, using previously established protocols (37). Individual clones were expanded and tested for activity by flow cytometry for the induction of *DsRed* gene expression and fluorescence after I-SceI plasmid transfection.

The ddSceGR plasmid was stably integrated into U2OS EJ-DR cells by nucleofection, followed by selection in G418 antibiotics for ~2 weeks. Single cell clones again were isolated by limiting dilution, and individual clones were expanded, followed by testing for ligand-induced NHEJ and HR repair activity by flow cytometry. Ligand-induced DNA cleavage by ddSceGR was performed by adding the Shield1 and triamcinolone (TA) ligands at concentrations of 0.5–1 μM and 100 nM, respectively, to the cell cultures. Unless otherwise indicated, ligands were incubated in the cells for 24 h, followed by two washes with DMEM containing 10% FBS without ligands.

### DSB repair assays

Initially, DSBs were induced at the EJ-RFP and DR-GFP loci by plasmid nucleofection with pCBASce or an empty vector as a control, according to the manufacturer's recommendations. One million cells were typically nucleofected with 10 μg of vector, and cells were then plated immediately into 6-, 12- or 24-well dishes as appropriate. NHEJ and HR repair activity was assessed by quantification of the percentages of DsRed+ and GFP+ cells, respectively, using a FACScan flow cytometer (Becton, Dickinson and Company; BD) at the indicated times. Standard compensation techniques were used when GFP and DsRed were analyzed simultaneously to minimize spectral overlap. DsRed+, GFP+ and parental cells were used as controls for optimization, and the data were analyzed using FloJo (Tree Star, Inc.). Experiments were performed in either triplicate or quadruplicate, and error bars represent standard errors of the mean (SEM). For DSB repair experiments involving ddSceGR, the Shield1 and TA ligands were added to cell cultures to induce DSBs as described earlier in the text.

### Breakpoint analyses

The I-SceI site and flanking sequence at the Sce-TetR locus was amplified and digested with I-SceI enzyme *in vitro* using previously described protocols (32) using the primers: 5′-GTTACAATGATATACACTGTTTGA-3′ (forward) and 5′-GACTTAGTAAAGCACATCTAA AAC-3′ (reverse). For sequencing of the breakpoint junctions, PCR amplicons were gel-purified and cloned using a TOPO TA cloning kit (StrataClone PCR cloning kit, Agilent Technologies), followed by DNA sequencing. DNA sequences were aligned and analyzed using Lasergene software (DNAStar, Inc).

### siRNA studies

siGENOME SMARTpool duplexes targeting key DSB repair and control genes were purchased from Dharmacon and were reconstituted as 20 μM stock

solutions according to the manufacturer's specifications. In all, 100 pmol of each duplex pool was nucleofected into U2OS EJ-DRs cells at the indicated times. Each nucleofection was typically performed with 1 million cells per cuvette, and the cells were immediately plated into 12-well dishes at a concentration of 40 K cells per well.

### Cell cycle analysis

The cell cycle profiles of U2OS cells passaged under different cell culture conditions were assessed by propidium iodide (PI) staining followed by flow cytometry analysis, as described previously (38).

### IR survival assays

Clonogenic survival assays were performed as described previously (38).

### Western blot analyses

Western blotting was performed as described previously (39). Briefly, protein samples were loaded into polyacrylamide gels and subjected to sodium dodecyl sulfate/polyacrylamide gel electrophoresis. To detect the protein of interest, the membranes were incubated with antibodies recognizing the following proteins: DNA-PKcs (ab-1832, Abcam), LigIV (polyclonal rabbit antibody aliquot kindly provided by Dr David Shatz, Yale Medical School), XRCC1 (#2735, Cell Signaling Technology), LigIII (6G9, Santa Cruz Biotechnology, Inc.), CtIP (polyclonal rabbit antibody aliquot kindly provided by Dr Richard Baer, Columbia University), BRCA2 (Ab-1, CalBiochem), SMC1 (A300-055A, Bethyl Laboratories) and FKBP12 (#610808, BD). The FKBP12 antibody was used to detect the destabilization domain of ddSceGR. Goat anti-mouse IgG [heavy and light chain (H&L)] and goat anti-rabbit IgG (H&L) labeled with horseradish peroxidase conjugate were used as secondary antibodies (Santa Cruz Biotechnology). Bands were detected using the ECL chemiluminescence detection method (Amersham Biosciences) and exposure on X-ray film.

### Immunofluorescence microscopy

Cells were seeded into eight-chamber tissue culture slides (Fisher) and incubated overnight, and selected slides were then treated with ionizing radiation using a Cesium Irradiator to deliver a dose of 10 Gy. A separate set of slides was irradiated after growth arrest by contact inhibition and serum deprivation, as presented in the 'Results' section. Cells were fixed in 4% paraformaldehyde at room temperature for 15 min, followed by a block and permeabilization step with 10% bovine growth serum and 0.5% Triton-X for 1 h. Commercially available antibodies were used to detect the following protein targets: phospho-specific γH2AX (S139; #32827, Upstate), phospho-specific DNA-PKcs (T2609; 10B1, Abcam), BRCA1 (D9, Santa Cruz Biotechnology), phospho-specific Chk2 (T68; #2661, Cell Signaling Technology) and GR (#PA1-511A, Thermo Scientific). The GR antibody was used to detect the GR domain in cells transfected with ddSceGR. The secondary antibodies used were Alexa Fluor 594-labeled goat anti-mouse IgG (Molecular Probes) and Alexa Fluor 488-labeled chicken anti-rabbit IgG (Molecular Probes), each at a 1:500 dilution. Cell nuclei were stained with 4′,6-diamidino-2-phenylindole, which was included in the Vectashield mounting medium (Vector Laboratories). Images were obtained using a Carl Zeiss confocal laser-scanning microscope (Carl Zeiss Microscopy, LLC) and processed using ImageJ and Adobe Photoshop software. For foci quantification, >100 nuclei were counted, with cells forming more than five foci scored as positive. Experiments were performed in either triplicate or quadruplicate, and error bars represent SEM.

## RESULTS

### Initial design and development of EJ-RFP to measure mutagenic NHEJ

We sought to develop an assay, which could monitor mutagenic NHEJ events in a robust and reproducible manner in living cells. We based our system on the tetracycline operon, which consists of a TetR protein that binds to tet operator (tetO) DNA sequences at selected target gene promoters, leading to repression of gene expression. Tetracycline binds TetR with high affinity, inducing a conformal change in the DNA binding domain of the protein. This change prevents binding to the tetO sequences with consequent expression of the target genes (40). This regulatory circuit can be used to control the expression of a gene of interest in mammalian cells, and numerous commercially available TetR-based systems have been reported previously (41).

We hypothesized that this regulatory circuit also could serve as a useful reporter for mutagenic NHEJ repair. As shown in Figure 1A, an I-SceI site was inserted into the 5′-end of the *TetR* gene in-frame, between the ATG start codon and the ORF of the gene. This construct serves as the NHEJ repair substrate, and it is referred to as Sce-TetR. In addition, we cloned a *DsRed* gene into a CMV-driven expression plasmid containing intervening tetO sequences, which serves as the reporter gene, and it is referred to as TO-DsRed (Figure 1A). When the repair substrate and reporter vector are chromosomally integrated in cells, *DsRed* gene expression is basally repressed by the TetR protein. In this system, a site-specific DSB can be induced at the Sce-TetR locus by expression of I-SceI. Subsequent rejoining of the free DNA ends by error-prone NHEJ results in disruption of the *TetR* ORF and consequent de-repression of *DsRed* gene expression. This NHEJ activity then can be assessed by flow cytometric analysis of DsRed fluorescence in living cells. DsRed and RFP will be used interchangeably in this manuscript. This system is referred to as the end-joining RFP (EJ-RFP) assay. As alluded to earlier, the various NHEJ sub-pathways have been given multiple names, each with potentially overlapping functions. In this article, alternative end-joining pathways collectively are non-canonical or mutagenic NHEJ repair. Furthermore, precise re-ligation of the I-SceI site is predominantly a cNHEJ-dependent process, as studies have clearly shown

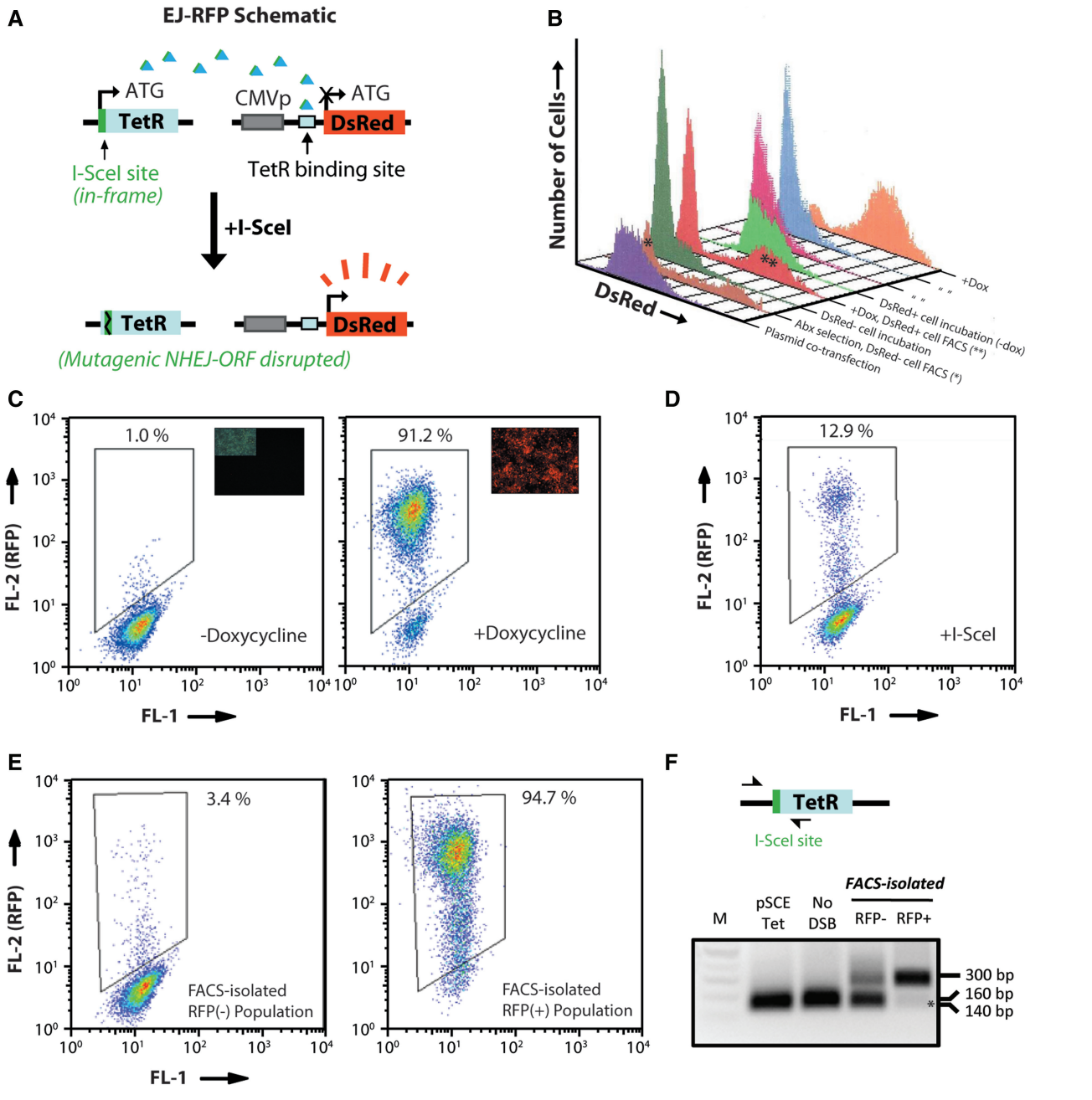


**Figure 1.** Initial design, development and characterization of EJ-RFP as an assay for mutagenic NHEJ repair. (**A**) EJ-RFP schematic depicting the cassettes from the NHEJ repair substrate and the *DsRed* reporter gene plasmids (Sce-TetR and TO-DsRed, respectively), which were engineered from a commercially available tet-on regulatory plasmid set (see 'Materials and Methods' section for details). Cleavage at the I-SceI site in the TetR plasmid can disrupt the ORF resulting in loss of TetR binding to its recognition sequence in the reporter gene plasmid, with consequent *DsRed* gene expression. (**B**) Novel FACS-based strategy to rapidly isolate cells with intrachromosomally integrated repair substrate and reporter gene plasmids. DsRed fluorescence intensity histograms are presented in a staggered offset format and in chronological order. The Sce-TetR and TO-DsRed plasmids were co-transfected into RKO cells and analyzed by flow cytometry after 2 days in culture (purple histogram), which revealed low

(continued)

that it is dependent on Ku70, XRCC4 and DNA-PKcs (22,32). Thus, our assay reports on the activity of the non-canonical NHEJ repair pathways.

After engineering the repair substrate and the reporter vectors, we sought to confirm that the additional I-SceI site sequence did not disrupt TetR protein function. To this end, either Sce-TetR or TetR plasmids were co-transfected transiently along with the TO-DsRed reporter gene vector into RKO colorectal cancer cells, followed by measurement of *DsRed* fluorescence by flow cytometry. These studies confirmed there were no significant differences in the repression of *DsRed* gene expression between the Sce-TetR and TetR proteins, suggesting that this approach would be feasible (data not shown).

### Development of polyclonal EJ-RFP cell lines with robust functional NHEJ reporter activity

*DsRed* expression also can be transiently induced in the EJ-RFP system by the addition of tetracycline, which reversibly disrupts binding by the TetR protein to the tetO sequences in the reporter vector via the mechanism described earlier in the text. This specific feature of the EJ-RFP assay facilitates the rapid isolation of cell lines with stably integrated copies of both plasmids, using FACS. Specifically, the Sce-TetR and TO-DsRed vectors can be linearized and co-transfected into cells, followed by antibiotic selection to enrich for cells containing chromosomally integrated copies of both plasmids. First, an initial FACS step is performed to isolate DsRed− cells after plasmid transfection and dual antibiotic selection. These isolated cells are likely to contain a population of cells with integrated functional copies of both Sce-TetR and TO-DsRed (i.e. such cells would contain an intact 'tetracycline regulatory loop'). Next, tetracycline (or the semi-synthetic analog doxycycline) is added to the culture medium to reversibly induce *DsRed* expression in these isolated cells. FACS is then performed once again to isolate DsRed+ cells. These cells are then washed and further incubated until *DsRed* expression is again repressed by Sce-TetR (in the absence of tetracycline). Such cells would be expected to have an intact tetracycline regulatory loop, and they could then be tested for I-SceI-induced DSB repair activity. Importantly, this approach obviates the need for sequential plasmid transfection, selection and single cell cloning.

We used the approach described earlier in the text to rapidly create an RKO cell line containing the EJ-RFP assay. As shown in Figure 1B, RKO cells were co-transfected with Sce-TetR and TO-DsRed followed by antibiotic selection. A distinct population of DsRed− cells was identified after ~1 week of antibiotic selection, and these cells were isolated by FACS. The isolated cells were then treated with doxycycline for 24 h, which induced high levels of DsRed expression in a sub-population of cells. These DsRed+ cells were isolated by FACS and then cultured for ~1 week in the absence of doxycycline, to allow re-repression of *DsRed* gene expression by Sce-TetR. As shown in Figure 1B and C, we obtained a relatively pure population of cells with doxycycline-inducible DsRed expression using this novel FACS-based selection approach. DsRed fluorescence was undetectable in these cells (in the absence of doxycycline), as assessed by both flow cytometry and epifluorescence microscopy, using parental RKO cells as a reference (data not shown and inset panels, Figure 1C). This cell line was named RKO-EJ.

Next, we sought to test the effects of DSB induction at the Sce-TetR locus on DsRed expression in RKO-EJ cells. As shown in Figure 1D, we detected a significant induction in the percentage of DsRed+ cells (12.9%) after nucleofection with an I-SceI expression vector. Cells were cultured in tetracycline-free media for all I-SceI transfections in this study. The percentage of DsRed+

**Figure 1.** Continued
levels of DsRed fluorescence. Cells were analyzed again after 1 week in antibiotic selection to enrich for RKO cells with intrachromosomally integrated plasmids, which revealed two distinct DsRed− and DsRed+ cell populations (brown histogram). The DsRed− population (indicated by an asterisk) was isolated by FACS and confirmed to contain predominantly DsRed− cells by flow cytometry one day after sorting (green histogram). Doxycycline was added to these cells for 24 h, which induced a DsRed+ population (red histogram; DsRed+ population indicated by double asterisks), and these cells were isolated by FACS. The isolated cells were then washed and incubated in culture medium without doxycycline for ~1 week to allow reconstitution of DsRed repression by Sce-TetR. These cells were analyzed every 2 days to measure residual DsRed fluorescence, which steadily declined during this time (green, pink and blue histograms). Doxycycline was once again added for 24 h to these cells, which induced DsRed expression in the majority of the cells (orange histogram), indicating successful enrichment of cells containing stably integrated functional copies of the Sce-TetR and TO-DsRed plasmids. This polyclonal cell line was referred to as RKO-EJ. (**C**) Confirmation of doxycycline-inducible DsRed expression in RKO-EJ cells isolated in (**B**), as detected by flow cytometry. Graphs represent bivariate histograms of DsRed fluorescence (*y*-axis) versus the FL-1 channel (*x*-axis) to facilitate the visualization of individual cells. Inset panels show representative epifluorescence microscopy images of DsRed fluorescence in RKO EJ cells 24 h after doxycycline treatment (a representative inset panel in the −doxycycline panel shows a light microscopy image confirming high cell density, which is apparent in the +doxycycline panel). (**D**) Detection of DsRed+ cells after I-SceI transfection in RKO-EJ cells. RKO-EJ cells were transfected with an I-SceI expression vector to induce a DSB at the Sce-TetR locus, followed by flow cytometry analysis after 96 h. (**E**) Sample flow cytometry plots for DsRed− and DsRed+ cells isolated 2 weeks after I-SceI plasmid transfection. Genomic DNA was isolated from these cells for analysis of the breakpoint by PCR amplification and DNA sequencing later in the text. (**F**) PCR amplification and *in vitro* restriction digestion analysis of PCR amplicons from the breakpoint junction at the Sce-TetR locus. Schematic depicting the approximate locations of the PCR primers in the locus is shown earlier in text. Agarose gel shows complete digestion of PCR amplicon generated from Sce-TetR plasmid template DNA using I-SceI (pSce Tet lane). Similar results were obtained with genomic DNA isolated from RKO EJ cells (no DSB lane), and these two lanes serve as controls to confirm that our enzymatic conditions are optimized for complete digestion of product. The majority of the PCR amplicons generated from RFP− cell genomic DNA are cleaved by I-SceI, suggesting that minimal mutagenic NHEJ events have occurred in this cell population (RFP− lane). In contrast, the PCR amplicons from the DsRed+ cells are almost completely resistant to digestion with I-SceI, suggesting that mutagenic repair events have occurred in the DsRed+ cells. Colors on the gel have been inverted for clarity. Asterisk indicates that the two cleavage bands are closely spaced and thus may appear as a single band on the gel. (**G**) DNA sequence analysis and alignment of the breakpoint in individually cloned Sce-TetR alleles isolated from unsorted cells after I-SceI plasmid transfection to induced DSBs. The consensus I-SceI sequence and site of cleavage in the Sce-TetR locus is shown for reference (highlighted in red and blue text). Sequence deletions are indicated by a dashed line, sequence insertions are indicated in green text and regions of microhomology are underlined for reference.

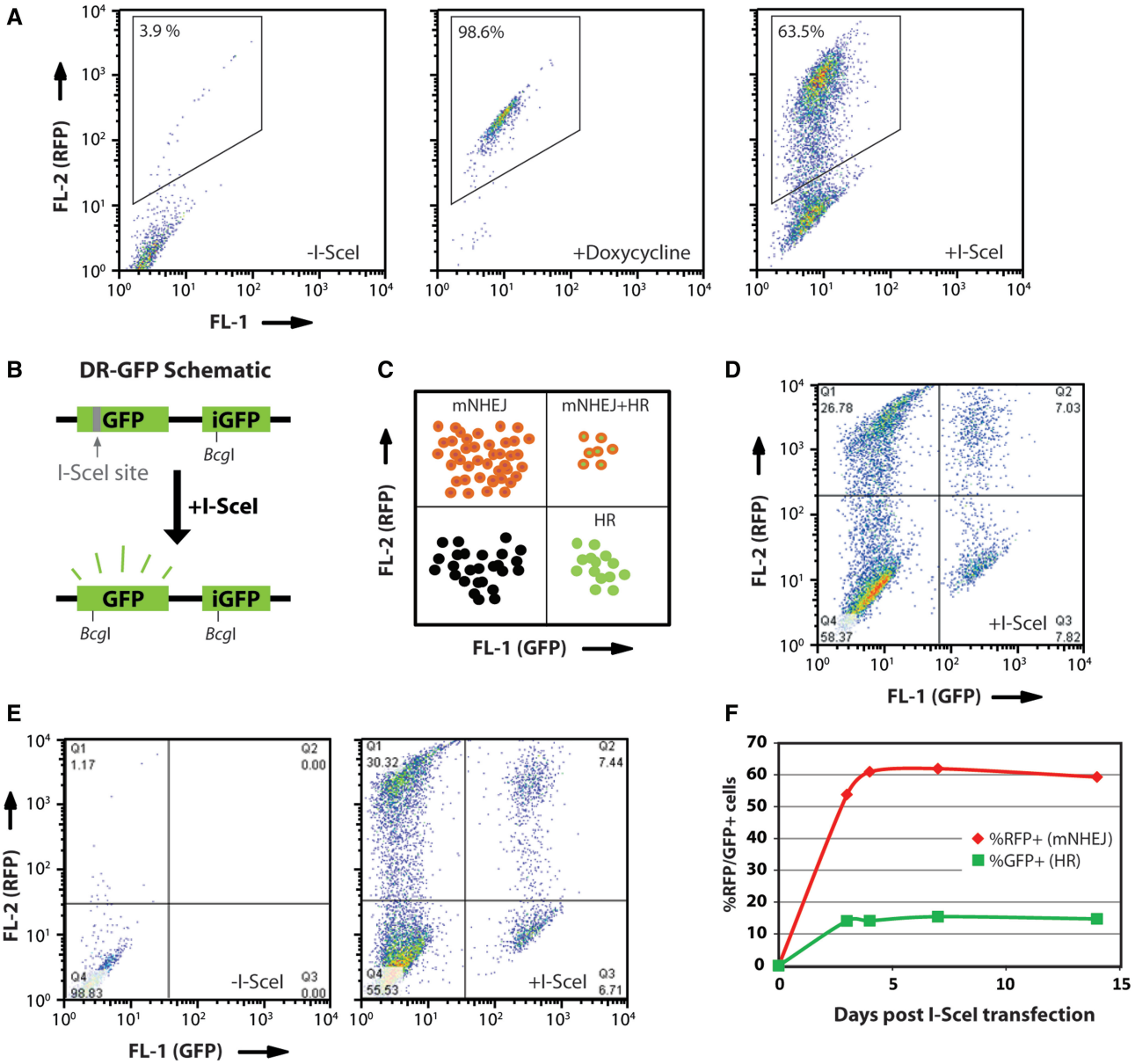


**Figure 2.** Creation of other EJ-RFP cell lines and combination with DR-GFP, an assay for homologous recombination. (**A**) Introduction of the EJ-RFP system into the glioma cell line, M059K, using the FACS-based enrichment approach described in Figure 1B. Representative flow cytometry plots are shown: low levels of DsRed+ cells in log-phase M059K-EJ cells (left), with high levels of DsRed+ cells after doxycycline exposure (middle) and a substantial increase in the percentages of DsRed+ cells are observed after transfection with an I-SceI plasmid (right). (**B**) Schematic of the previously described DR-GFP assay to measure HR in cells at an intrachromosomal site (21). (**C**) Schematic of the readout that would be obtained from a cell line containing integrated copies of both the EJ-RFP and DR-GFP assays, in which mutagenic NHEJ (mNHEJ) is detected as an increase in DsRed+ cells and HR is detected as in increase in GFP+ cells. The assays each report on DSB repair activities at separate loci; thus, it would be possible to detect cells in which both mNHEJ and HR repair events have occurred (which would appear as DsRed+ and GFP+, respectively). (**D**) Creation of U2OS EJ-DR cells, containing stable copies of both DSB repair assays as described in (C). A bivariate flow cytometry histogram of DsRed fluorescence (*y*-axis) versus GFP fluorescence (*x*-axis) is shown representing mNHEJ and HR, respectively, 96 h after transfection with an I-SceI plasmid to induce DSBs. This cell line was created using the FACS-based enrichment approach described in Figure 1B. A substantial increase in the percentages of both DsRed+ and GFP+ cells is observed after I-SceI plasmid transfection, indicating robust levels of mutagenic NHEJ and HR repair, respectively. Low levels of DsRed/GFP+ cells were observed in the absence of DSB induction, as shown later in (E). (**E**) Isolation of a U2OS EJ-DR single cell clone with low background levels of fluorescent protein expression (left), which is inducible on I-SceI plasmid transfection followed by analysis after 96 h (right). (**F**) Time course analysis of the levels of DsRed+ and GFP+ cells after I-SceI plasmid transfection in a representative U2OS EJ-DR single cell clone, corresponding to mNHEJ and HR repair, respectively, as detected by flow cytometry.

cells reached a maximum at ~96 h after I-SceI nucleofection, and it was stable at multiple distant time points (e.g. 1–2 weeks post-transfection; Figure 2F and data not shown). Furthermore, the ability to engineer this system into cells without the need for single cell cloning is a key advantage of this system. We also created single cell clones of RKO-EJ by limiting dilution, and we confirmed robust and reproducible percentages of DsRed+ cells after DSB induction with I-SceI in these clones (data not shown).

To confirm that DsRed expression indeed was the result of TetR ORF disruption by error-prone NHEJ repair at the Sce-TetR locus, we isolated pure populations of DsRed+ and DsRed− cells after DSB induction, followed by an analysis of the I-SceI site breakpoint by PCR and *in vitro* restriction digestion. Sample flow cytometry profiles of the isolated DsRed− and DsRed+ cells are shown in Figure 1E, and we confirmed that the two cell populations retained their respective DsRed expression levels at multiple time points after the initial FACS isolation >2 weeks (data not shown). Genomic DNA was extracted from these two cell populations, and the region containing the I-SceI site in the Sce-TetR locus was amplified by PCR. The PCR products were then treated with I-SceI enzyme *in vitro* to assess the integrity of the I-SceI site in the isolated DsRed+ and DsRed− cells. Cleavage-resistant bands *in vitro* would indicate that mutagenic repair had occurred *in vivo*. As shown in Figure 1F, the PCR products from the DsRed+ cells were resistant to I-SceI digestion, which indicated that sequence changes at the Sce-TetR locus had occurred in these cells, resulting in DsRed expression. I-SceI digestion of PCR products amplified either from the Sce-TetR plasmid or from RKO-EJ cells in which no DSB had been induced (i.e. cells transfected with an empty vector instead of an I-SceI plasmid) resulted in 100% fragment cleavage, which served as a positive control for optimized restriction digestion conditions (Figure 1F). These data support the conclusion that DsRed expression after I-SceI transfection is caused by mutagenic NHEJ repair events, which disrupt the ORF of Sce-TetR. Interestingly, a small proportion of PCR products amplified from the DsRed− cell population also was resistant to cleavage by I-SceI, suggesting mutagenic NHEJ events had occurred in cells which did not disrupt the Sce-TetR ORF, thus maintaining repression of *DsRed* expression (e.g. these likely represent in-frame insertions or deletions).

Next, we cloned and sequenced individual PCR products from RKO-EJ cells after I-SceI expression to further confirm and study the spectrum of mutagenic NHEJ repair events at the Sce-TetR locus. Genomic DNA was extracted from unsorted RKO-EJ cells after DSB induction, which was then pre-digested with I-SceI *in vitro* to enrich for mutated PCR products. As shown in Figure 1G, we detected a wide range of characteristic NHEJ events, including insertions, deletions and deletions with microhomology usage. Taken together, these data suggest that the EJ-RFP system can be used to monitor mutagenic NHEJ in cells at an intrachromosomal locus in a robust and reproducible manner.

### Creation of other EJ-RFP cell lines and combination with DR-GFP, an assay for homologous recombination

Based on our success in rapidly creating the RKO-EJ cell line, we engineered several other EJ-RFP cell lines using our FACS-based enrichment strategy. To this end, we integrated the Sce-TetR and TO-DsRed plasmids into the malignant glioma cell line, M509K, and we confirmed substantial percentages of induced DsRed+ cells after I-SceI transfection in polyclonal cell lines, ranging between 30 and 40% (data not shown). This cell line was named MK-EJ. Single cell MK-EJ clones were also derived with high levels of mutagenic NHEJ repair. An example is shown in Figure 2A, in which induced DsRed+ percentages reached ~64% after I-SceI transfection.

Next, we tested whether we could combine the EJ-RFP system with an assay for HR, such that these two key DSB repair pathways could be assessed simultaneously in living cells. We chose to use the DR-GFP HR assay for these studies (21). A schematic of this assay is presented in Figure 2B for reference. The DR-GFP assay has been integrated into U2OS cells previously, and high levels of HR activity have been reported in this cell line (36), which we refer to as the U2OS DR cell line. We integrated the EJ-RFP system into U2OS DR cells, again using the FACS-based enrichment strategy described earlier in the text to create a polyclonal cell line containing both reporter systems. This cell line was named U2OS EJ-DR. We postulated that I-SceI transfection in this cell line would result in four populations of cells based on DsRed and GFP expression, corresponding to NHEJ and HR repair, respectively. A schematic of the expected results is shown in Figure 2C. Indeed, we detected substantial percentages of induced DsRed+ and GFP+ cells after I-SceI transfection in FACS-isolated, polyclonal U2OS EJ-DR cells (Figure 2D). Low levels of %GFP+ and %DsRed+ cells were identified in mock-transfected cells (~3 and 0.5%, respectively; data not shown). Similar results also were obtained in several single cell clones of U2OS EJ-DR (Figure 2E and data not shown). A time course analysis revealed that the percentages of DsRed+ and GFP+ cells peaked at 96 and 72 h, respectively, in these single cell clones, and these percentages remained stable for prolonged periods after I-SceI transfection (Figure 2F; representative single cell clone, which is notable for high levels of induced mutagenic NHEJ repair). In theory, prolonged unrepaired DSBs could temporarily disrupt Sce-TetR expression (e.g. by preventing transcription at the gene locus). Reduced Sce-TetR expression in turn could transiently de-repress DsRed expression, leading to potential false-positive results suggestive of NHEJ repair activity. However, as shown in Figure 2F, we did not observe any transient increases in DsRed expression at early time points (e.g. 72 h; also shown in Supplementary Figure S1A), and DsRed expression in positive cells remained stable for >2 weeks. In subsequent experiments, we have cultured U2OS EJ-DR cells for >3 months after DSB induction, with minimal changes in the percentages of GFP+ and DsRed+ cells (data not shown). Finally, we also performed a series of cell mixing experiments with FACS-isolated GFP+ and DsRed+ cell populations, which confirmed that there were no overlapping fluorescence patterns, as this could otherwise confound the simultaneous detection and analysis of both fluorescent proteins (data not shown). This is particularly relevant given a recent report that immature DsRed fluorescent proteins can transiently display strong green fluorescence (42). In summary, these data suggest that combining EJ-RFP with

an HR assay is feasible, and that it can serve as a robust and reliable reporter to monitor both the NHEJ and HR pathways in living cells.

### Development of a novel system for ligand-inducible cleavage by I-SceI

During the course of these studies, we sought to develop a stably integrated version of an inducible I-SceI expression vector, which would obviate the need for transient transfection of I-SceI plasmids to induce the site-specific DSB. We reasoned that this would facilitate future siRNA experiments with our assay, as they typically require an initial transfection to deliver siRNAs, followed by a second transfection with I-SceI for DSB induction. We and others have found such serial transfections to be toxic to cells, and often they are associated with variable experimental results [data not shown (22)]. A modified I-SceI gene has been described, which was fused to a mutant form of the estrogen receptor (ER) ligand-binding domain on both the N- and C-termini. These domains confer ligand-dependent localization to chromosomal DNA, and cell lines were made with intrachromosomally integrated copies of this modified I-SceI gene. However, the levels of ligand-induced DSB induction were low, suggesting that the flanking ER domains may impair I-SceI cleavage function (22). The Misteli laboratory has developed a novel inducible I-SceI system, which consists of a fusion between the I-SceI gene and the ligand-binding domain of the rat GR on the C-terminus, which we refer to as SceGR (34). In the absence of the synthetic GR ligand, TA, SceGR is excluded from the nucleus such that DNA cleavage is limited. Addition of TA induces rapid protein translocation from the cytoplasm into the nucleus and consequent DSB induction, which is reversible on withdrawal of the ligand. This system permits substantial control of I-SceI cleavage rates, although low levels of DSB induction can be detected in the absence of ligands (34). Such 'leakiness' can be minimized by culturing cells in charcoal-stripped FBS, which removes naturally occurring glucocorticoids that are found in most FBS preparations. However, charcoal-stripped FBS can significantly impair cell proliferation and viability, likely because the stripping process also removes key growth factors, cytokines and other steroid hormones [Bindra *et al.*, unpublished results (43–46)].

Based on the findings discussed earlier in the text, we hypothesized that the addition of a ligand-dependent protein stability domain would provide an additional level of control to regulate DSB induction by I-SceI. A 'two-tiered' control of I-SceI cleavage (i.e. protein levels and nucleocytoplasmic localization) likely would facilitate the creation of cell lines with intrachromosomally integrated copies of this modified endonuclease, and we thought it may reduce the need for continuous culture in charcoal-stripped FBS. To this end, we added a destabilizing domain (dd) derived from the FKBP12 protein to the N-terminus of Sce-GR. This modified fusion protein is referred to as ddSceGR. The addition of the drug, Shield1, blocks the destabilizing effect of the N-terminal domain, resulting in a rapid increase in protein levels. This system was developed by the Wandless laboratory (47), and it is now commercially available as the ProteoTuner system (Clontech Laboratories, Inc.). As an initial test, we transiently transfected the ddSceGR vector into U2OS EJ-DR cells, followed by western blot analysis and confocal immunofluorescence microscopy in the presence or absence of the Shield1 and TA ligands. Antibodies specific to the FKBP12 and GR domains were used to detect ddSceGR expression in these studies. As shown in Figure 3A and B, ddSceGR protein levels were substantially higher in the presence of ligands, as detected by both western blot and confocal microscopy analysis. Furthermore, ddSceGR protein was predominantly localized to the nucleus in these cells after ligand addition (Figure 3B and Supplementary Figure S1F). Next, we assessed the rates of ligand-induced cleavage indirectly by measuring HR after transient transfection with ddSceGR in U2OS DR cells. Cells were incubated in ligands for 24 h immediately after ddSceGR nucleofection, followed by two washes with culture medium that did not contain TA/Shield1, and then analyzed by flow cytometry after an additional 72 h. As shown in Figure 3C, minimal percentages of GFP+ cells were detected 72 h after ddSceGR transfection in the absence of ligands (0.3% GFP+ cells). In contrast, the addition of ligands induced a significant increase in ddSceGR-induced HR activity (7.1% GFP+ cells, representing an almost 25-fold increase in repair compared with the control cells). The addition of the N-terminal dd domain reduced the overall cleavage activity of I-SceI by ~30% compared with SceGR (Supplementary Figure S1B). However, it reduced background cleavage activity in the absence of ligands by >3-fold. Thus, the addition of both domains significantly enhanced the relative inducibility of cleavage rates under these conditions.

The data presented earlier in the text suggested that our novel modifications to the I-SceI protein would make it suitable for intrachromosomal integration in cell lines. To this end, we integrated ddSceGR into a single cell U2OS EJ-DR clone by plasmid nucleofection and using standard cloning techniques. We isolated and tested several single cell clones containing ddSceGR, and one representative clone is shown in Figure 3D. We refer to these cells as U2OS EJ-DRs cells. Low percentages of GFP+ and DsRed+ cells (corresponding to HR and mutagenic NHEJ repair, respectively) were observed in the absence of ligands in the majority of the isolated single cell clones, and these levels increased significantly after a 24-h exposure to ligands (Figure 3D and E). Importantly, minimally increased levels of ddSceGR-induced DSB repair were detected when each ligand was added separately (Figure 3E). Low background levels of GFP+ and DsRed+ cells were observed in untreated cells for extended time points in continuous culture, and the ligand-induced levels of HR and mutagenic NHEJ repair were stable over time after a 24-h exposure to ligand (Figure 3F and data not shown). Incubation with both ligands consistently resulted in maximal repair activity, highlighting the importance of both domains in

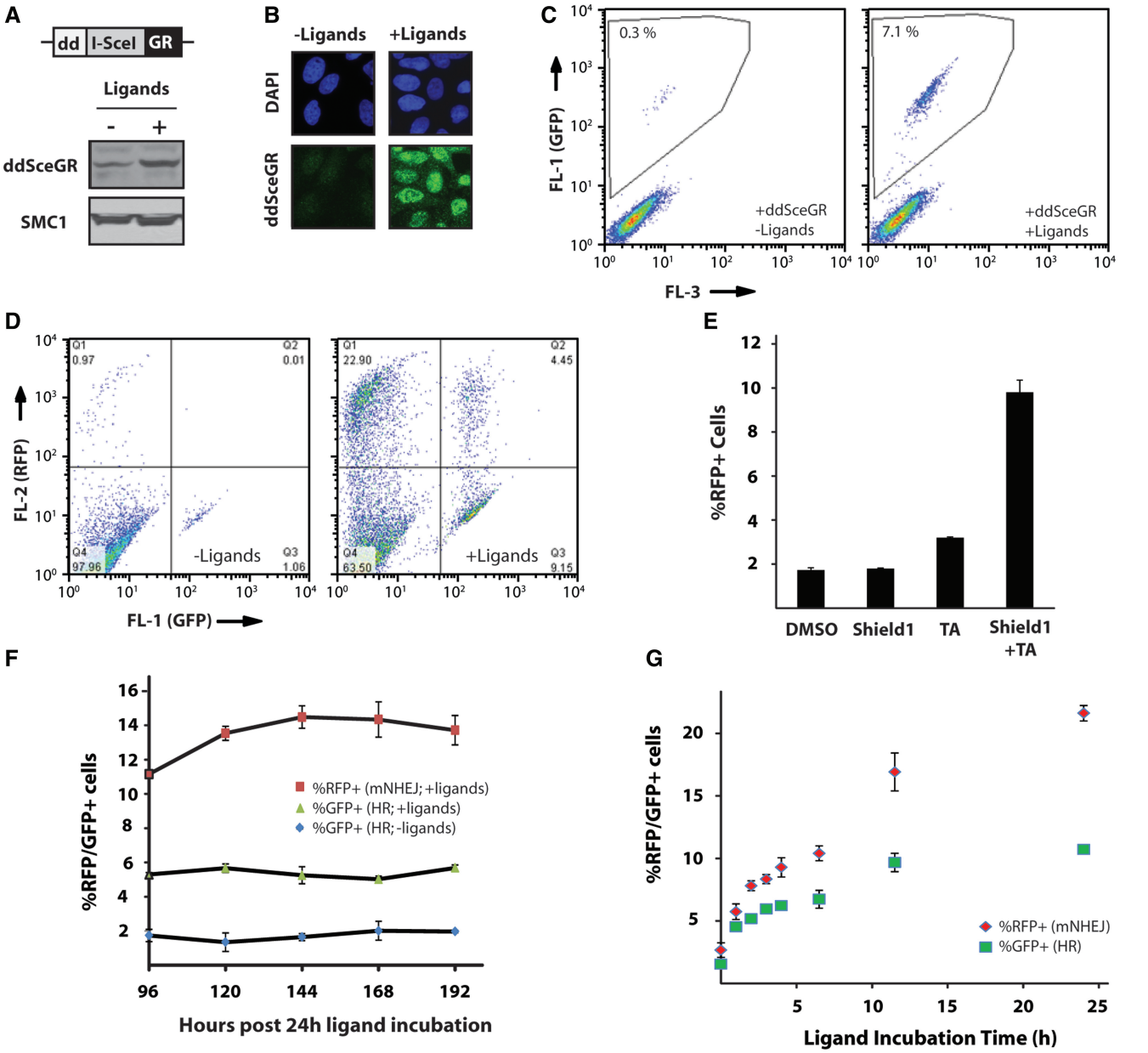


**Figure 3.** Development of a novel system for ligand-inducible cleavage by I-SceI. (**A**) Creation of a novel I-SceI fusion protein with an N-terminal ligand-dependent dd and a C-terminal GR ligand-binding domain, which we have named ddSceGR (schematic shown in top). These domains induce protein stability and nuclear localization in the presence of the ligands Shield1 and TA, respectively. Induction of ddSceGR protein expression levels was confirmed by western blot analysis with an antibody specific to the dd (lower). SMC1 is shown as a loading control for reference. (**B**) Confirmation of ligand-induced protein stability and nuclear localization by confocal microscopy in U2OS EJ-DR cells transiently transfected with a ddSceGR plasmid in the presence or absence of Shield1 and TA ligands (1 μm and 100 nm, respectively). The ddSceGR protein was detected using an antibody specific to the GR domain, and images were taken 24 h after transfection and ligand addition. (**C**) Ligand-dependent control of DSB induction, as detected by HR repair in U2OS DR cells after transfection with ddSceGR. Immediately after transfection, U2OS DR cells were equally split into two plates; Shield1 and TA ligands were added to one plate (with vehicles alone added to the other plate), and the GFP+ cells were assessed by flow cytometry at 72 h. (**D**) Creation of a U2OS EJ-DR single cell clone containing stably integrated ddSceGR, which we have named U2OS EJ-DRs. Representative flow cytometry plots for a U2OS EJ-HRs single cell clone demonstrating low levels of DsRed+ and GFP+ cells in the absence of Shield1 and TA ligands, which is highly inducible after a 24-h exposure to the ligands. (**E**) Robust ligand-dependent DSB induction and consequent NHEJ repair requires both Shield1 and TA ligands. U2OS EJ-DRs cells were exposed to vehicle alone (DMSO), Shield1 alone, TA alone or both ligands for 24 h, followed by flow cytometric analysis of DsRed+ cells after 96 h to measure induced mNHEJ repair. Experiments were performed in duplicate, and error bars represent standard deviations. (**F**) Stability of induced DsRed+ and GFP+ cell percentages in U2OS EJ-DRs cells after a 24-h incubation with Shield1 and TA ligands, as detected by flow cytometry at 24-h intervals (starting at 96 h after ligand exposure). (**G**) Analysis of the effects of Shield1 and TA ligand incubation time on induced mNHEJ and HR repair rates. U2OS EJ-DRs cells were incubated with ligands for the indicated periods followed by media washing and analysis of DsRed+ and GFP+ cells after 96 h to measure induced mNHEJ and HR repair, respectively. Data points at the y-intercept reflect treatment with vehicle alone (DMSO). Experiments were performed in triplicate, and error bars represent SEM.

ddSceGR regulation (Supplementary Figure S1C and D). Intriguingly, we observed a dose-dependent induction of DSB repair activity when the Shield1 concentration was varied between 10 and 500 μM but with a constant TA ligand concentration (100 nM; Supplementary Figure S1C). These data suggest that DSB activity can be 'tuned' using this system based on regulation of ligand-dependent protein stability.

We also tested the effects of shorter ligand exposure times on induced DSB repair. As shown in Figure 3G, ligand exposure time correlated closely with the percentages of induced DsRed+ and GFP+ cells. Remarkably, we detected substantial increases in these percentages even after a brief 1-h exposure to ligands, which highlights the exquisite control over ddSceGR cleavage rates using this approach. We have attributed this tight level of control to the use of regulatory mechanisms that are strictly post-translational (i.e. protein stability and nuclear localization). In support of this notion, recent studies have shown that SceGR is rapidly exported from the nucleus, within 1–2 h, after a media wash (48). In contrast, ligand incubation in U2OS EJ-HRs cells without media washing led to continuously increasing percentages of GFP+ and DsRed+ cells, which again highlights the ligand-dependent control of cleavage activity with this system (Supplementary Figure S1E). Collectively, these data support the use of the ligand-inducible ddSceGR system as a means to create a site-specific DSB without the need for plasmid transfection. Furthermore, another advantage of this system is that DSB cleavage kinetics can be precisely controlled by regulating activity at the level of both protein stability and nucleocytoplasmic localization, allowing brief periods of DSB induction.

### Validation of the EJ-DRs system in a focused siRNA-based study of key DSB repair genes

Next, we validated our combined dual repair assay and inducible I-SceI system in a focused study of key DSB repair genes. In this study, we sought to probe the relative roles of selected genes in both mutagenic NHEJ and HR repair, using a system that could uniquely detect dynamic shifts between the two pathways. U2OS EJ-DRs cells were nucleofected with siRNAs targeting selected DSB repair genes, followed by incubation between 48 and 72 h to allow time for downregulation of target gene expression. In parallel, cells were treated with siRNAs targeting either a scrambled sequence or a housekeeping gene (e.g. Glyceraldehyde 3-phosphate dehydrogenase; GAPDH) as negative controls. Cells were then treated with Shield1 and TA for 24 h to induce DSBs, followed by washing to remove ligands and analysis by flow cytometry after an additional 96 h. The percentages of DsRed+ and GFP+ cells transfected with siRNAs targeting the DSB repair genes were normalized to the percentages observed in cells transfected with control siRNAs for both mutagenic NHEJ and HR, respectively. In this manner, the data can be presented as a relative assessment of DSB repair on a 2D plot (which we refer to as a RADAR plot), which allows one to rapidly assess the effects of a given siRNA knockdown on both mutagenic NHEJ and HR repair activity. A schematic of how these data are presented is shown in Figure 4A.

The results of this focused DSB repair gene study are shown in Figure 4B. Data are also presented in this figure for cells treated under altered growth conditions, which will be described in the next section later in the text. Representative western blots are also shown in Figure 4C and Supplementary Figure S1G, which confirmed significant levels of target gene knockdown for the majority of the siRNAs tested. As expected, siRNA-induced downregulation of the key recombinational repair genes, *BRCA1* and *BRCA2* resulted in substantial reductions in HR repair activity, with minimal effects on mutagenic NHEJ, which is consistent with previous studies (49). In contrast, downregulation of the key cNHEJ genes, *DNA-PKcs*, *Ku80*, *XRCC4* and *LigIV*, resulted in a significant increase in both HR and mutagenic NHEJ. The findings of increased HR in response to abrogation of the cNHEJ pathway have been reported previously (32,50–54). In addition, the findings of increased mutagenic NHEJ in the EJ-RFP assay after cNHEJ repression highlight the dynamic balance between cNHEJ and mutagenic NHEJ pathways, as the former pathway clearly seems to predominantly favor simple re-ligation of cohesive DSBs without sequence alteration (22,32,55).

As mentioned earlier, controversy exists over the specific proteins involved in the more mutagenic non-canonical NHEJ pathways. We thus tested the effects of siRNA knockdown of genes previously implicated in non-canonical NHEJ repair, including *LigIII*, *XRCC1* and *PARP1*, on HR and mutagenic NHEJ repair in our assay. We also tested siRNAs targeting the *LigI* gene, based on previous studies suggesting functional redundancies between *LigI* and *LigIII* (12,56). Surprisingly, downregulation of these genes did not significantly affect mutagenic NHEJ (and no effects were seen on HR, as expected; Figure 4B). Our siRNA treatments induced substantial decreases in protein levels for these genes, which suggest that our data cannot be explained by incomplete siRNA-mediated knockdown (Figure 4C and data not shown). *CtIP* seems to play an important role in HR (57), and recent studies suggest that this protein also promotes certain types of mutagenic NHEJ (22,58). As expected, *CtIP* knockdown was associated with a decrease in HR repair levels, albeit these reductions were lower than what was observed in the case of *BRCA1* and *BRCA2* knockdown. Interestingly, *CtIP* knockdown did not result in impaired mutagenic NHEJ. In contrast, we observed slightly increased levels of mutagenic NHEJ under these conditions (Figure 4B). *CtIP* knockdown sufficiently attenuated protein expression levels, as we observed an HR phenotype in these same cells at the DR-GFP locus, and western blot analyses indicated low levels of CtIP protein after siRNA treatment (Figure 4C). These data suggest that CtIP may play a limited role in promoting mutagenic NHEJ repair [in contrast to previous reports (22)], and if anything could suppress this pathway.

Taken together, the data presented earlier in the text validate the EJ-RFP system as a valid reporter of mutagenic NHEJ repair, and they highlight the use of both the

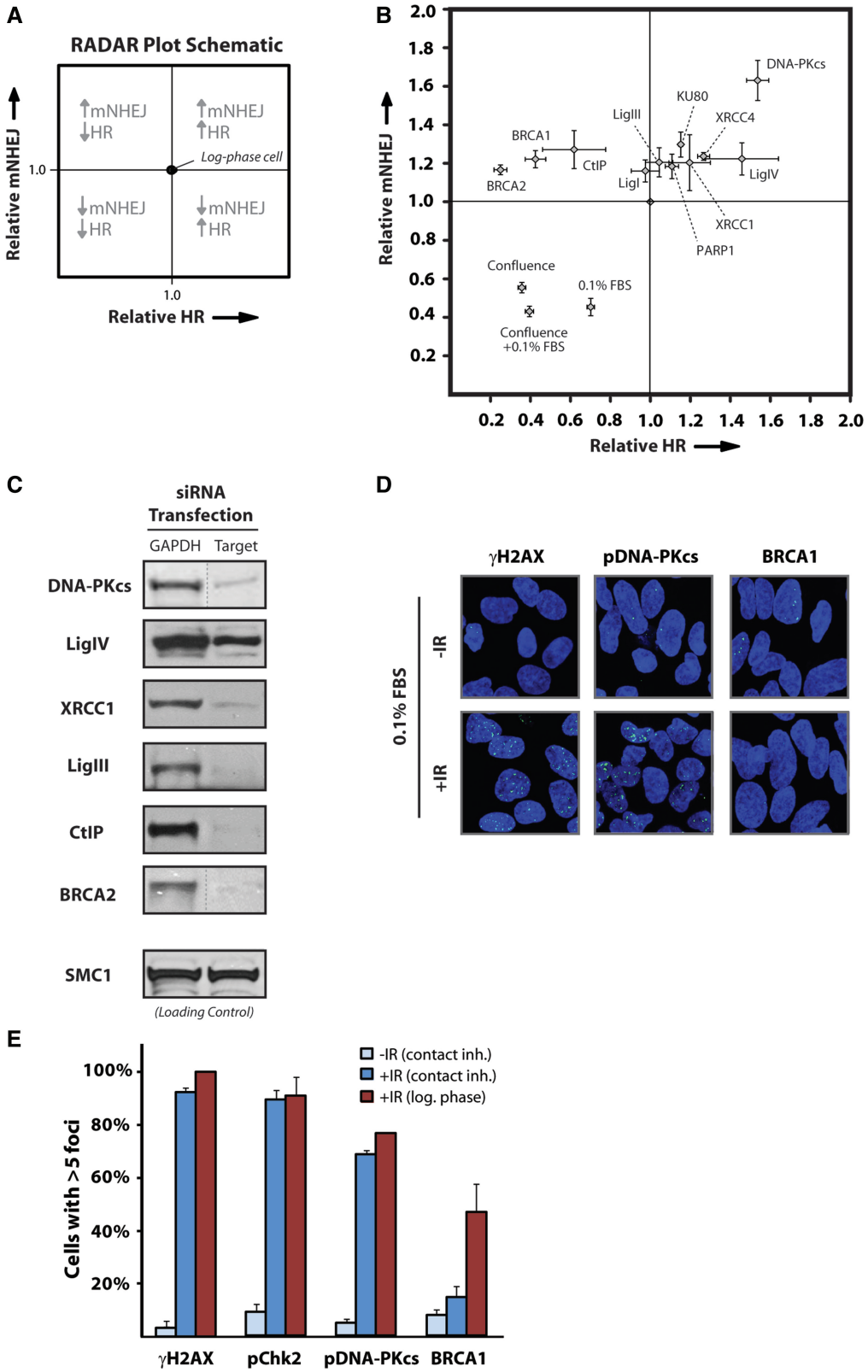


**Figure 4.** Validation of the EJ-DRs system in a focused siRNA-based study of key DSB repair genes and a growth-arrest study. (**A**) Schematic of data presentation format for siRNA and growth studies, referred to as a relative assessment of DSB repair (RADAR) plot. Rates of mNHEJ and HR repair, as detected by flow cytometric analysis of DsRed+ and GFP+ cells, respectively, for a given siRNA treatment or growth condition are normalized to that obtained from control cells after transfection with a scrambled siRNA sequence (indicated by black dot in center of plot). Potential effects on DSB repair pathways are shown in each quadrant for reference. (**B**) RADAR plot analysis of U2OS EJ-DRs cells after treatment with the indicated siRNAs or cell growth conditions. Experiments were performed in triplicate or quadruplicate, and error bars represent SEM. (**C**) Representative western blots from U2OS EJ-DRs cells treated with the siRNAs targeting the indicated proteins, demonstrating substantial

(continued)

assay and the inducible I-SceI system to study DSB repair patterns. The simultaneous measurement of both HR and mutagenic NHEJ repair in the EJ-DR system allows one to monitor dynamic shifts between these two pathways. In addition, simultaneous measurement can provide an internal control for selected phenotypes, as illustrated in the *CtIP* siRNA studies.

### Mutagenic NHEJ is repressed in growth-inhibited cells

During the course of ddSceGR testing, it became apparent that mutagenic NHEJ repair activity specifically was suppressed in U2OS EJ-DRs cells cultured in charcoal-stripped serum, with minimal effects on HR (data not shown). Stripped serum is known to contain reduced levels of growth factors, cytokines and endogenous steroids, and it often can impair cell proliferation in cell lines (43–46). In addition, previous reports have suggested that selected non-canonical NHEJ pathways are down-regulated in non-proliferating cells, whereas cNHEJ remains intact (10,16–18,59). However, most of the studies on non-canonical NHEJ repression only used pulse-field gel electrophoresis and γH2AX foci analyses; thus, further molecular studies are warranted to better elucidate this phenomenon. Based on these findings, we hypothesized that mutagenic NHEJ, as detected in our novel assay, may be repressed under growth-arrested and/or serum-deprived conditions. DSB induction by transient transfection with an I-SceI plasmid would not be technically feasible in growth-arrested or serum-deprived cells; therefore, we took at advantage of the ligand-inducible ddSceGR technology presented in this manuscript to directly address this question. To this end, cells were grown to 100% confluence and cultured for 4 additional days to induce arrest in the $G_0/G_1$-phase of the cell cycle. In one set of cells, the FBS concentration in the culture medium was also changed from 10 to 0.1% to further drive down active proliferation. These two conditions resulted in significant increases in the fractions of cells in the $G_0/G_1$-phase of the cell cycle, as confirmed by flow cytometric analysis of PI-stained cells ($G_0/G_1$-phase >75% in both sets of cells, Supplementary Figure S1H). DSBs then were induced by ligand exposure for 24 h, followed by flow cytometry analysis 72 h later to measure DSB repair. As expected, substantial decreases in HR repair activity were observed under these conditions, as this pathway is repressed in $G_0/G_1$ [Figure 4B (60)]. Intriguingly, mutagenic NHEJ was also substantially reduced under both conditions of growth arrest. Similar levels of ligand-induced ddSceGR protein levels and doxycline-induced DsRed fluorescence were observed in confluent versus log-phase cultures, as detected by western blot and flow cytometry analyses, respectively (Supplementary Figure S2A and B). Thus, these differences cannot be explained by impaired ddSceGR expression or repressed DsRed fluorescence under these conditions. Finally, it is well established that GR function and SceGR cleavage activity are retained in $G_0/G_1$-arrested and serum-deprived cells (including U2OS cells), which further support that ddSceGR is functional under these conditions (34,61,62).

In addition, we also tested a set of initially log-phase U2OS EJ-DRs cells cultured for 12–24 h in low-serum DMEM (0.1% FBS) before DSB induction with ligands for 24 h. This brief period of serum deprivation had modest effects on the cell cycle state of these cells (Supplementary Figure S1H). Previous studies have shown that this brief duration of serum deprivation adequately simulates growth factor withdrawal (63,64). Thus, we reasoned that this experiment might provide a better assessment of the effects of growth factor withdrawal specifically, rather than $G_0/G_1$ growth arrest, on mutagenic NHEJ repair activity. As shown in Figure 4B, less profound effects were observed on HR repair activity, which is consistent with a higher S-phase fraction than in the growth-arrested cells. In contrast, we again observed significant repression of mutagenic NHEJ repair, at levels similar to the results obtained in the fully growth-arrested cells. Collectively, these data suggest that mutagenic NHEJ is repressed by both $G_0/G_1$-arrest and serum deprivation. Importantly, these experiments also highlight the use of the EJ-DRs system to measure DSB repair pathway activity, especially under conditions where it is technically difficult to induce DSBs by I-SceI plasmid transfection.

To test whether cNHEJ was functional in $G_0/G_1$-arrested cells, we examined phosphorylated DNA-PKcs IR-induced foci under these conditions, and also in log-phase cells for comparison. The formation of DNA-PKcs foci at DSBs is a critical initial step for cNHEJ repair, and it seems to be mediated by the Ku70/80 proteins (65). As cNHEJ nears completion, DNA-PKcs is phosphorylated at multiple sites, including threonine 2609 and serine 2056, which is thought to eventually facilitate dissociation of DNA-PKcs from Ku70/80 and DNA [reviewed in (65)]. Inhibition of DNA-PK kinase activity with small molecules disrupts foci formation and is associated with profound radiosensitivity, indicating a critical role for this protein in cNHEJ (Supplementary Figure S2C and D). These findings suggest that it can be used as a surrogate for cNHEJ repair activity. As shown in Figure 4D and E, IR induced significant levels of γH2AX foci above background in both proliferating and arrested cells, which was expected, as DSBs would be induced in both conditions, regardless of the growth state of the cells. Furthermore, similar levels of IR-induced Chk2 and

**Figure 4.** Continued
knockdown of target genes. Cell extracts were isolated 72 h after siRNA nucleofection, and SMC1 is shown as a loading control for reference. (**D**) IR-induced DSB repair protein foci analysis in growth-arrested serum-deprived U2OS EJ-DRs cells. Cells were treated or not with IR (10 Gy) followed by incubation for 4 h, fixed and stained with antibodies targeting the indicated proteins and then analyzed by confocal microscopy. (**E**) Quantitation of DSB repair protein foci in U2OS EJ-DRs cells from (D); cells with >5 foci were scored as positive. Log-phase irradiated U2OS EJ-DR cells were also analyzed in parallel as a positive control to confirm robust foci-staining protocols. Experiments were performed in duplicate, and error bars represent standard deviations.

53bp1 foci formation were detected in both conditions (Figure 4E and data not shown, respectively), suggesting that proximal DSB repair signaling also was not altered in the growth-arrested cells. As expected, IR-induced BRCA1 foci formation was markedly reduced in arrested cells in comparison with log-phase, which is consistent with previous reports confirming that both BRCA1 expression and HR activity are significantly reduced in the $G_0/G_1$-phase of the cell cycle (60). The absence of BRCA1 foci in the cells after irradiation also serves as a control to confirm the growth-arrested state of the cells under these culture conditions. However, phosphorylated DNA-PKcs foci formation was largely intact in growth-arrested cells. Similar results were obtained with DNA-PKcs antibodies recognizing the ataxia telangiectasia mutated-dependent site, threonine 2609 (T2609), and an autophosphorylation site, serine 2056 [Figure 4D and E, and data not shown (65)]. Taken together, these data suggest that cNHEJ is functioning in growth-arrested cells, whereas mutagenic NHEJ is significantly repressed under these conditions.

## DISCUSSION

Here, we present the development of a novel NHEJ repair assay and a ligand-inducible system to control site-specific DNA cleavage in mammalian cells. Our NHEJ assay provides a robust and reproducible measure of mutagenic NHEJ repair, and it can be rapidly integrated into cell lines using a unique FACS-based enrichment strategy. Furthermore, we demonstrate that our NHEJ assay can be combined with an established HR assay to measure both pathways simultaneously in living cells. Our inducible DSB system is unique because it can be integrated into cell lines, with extremely high levels of cleavage-induced DSB repair, and also tightly controlled DSB induction rates. We have validated our combined DSB repair assay and inducible DSB system in a focused siRNA study of key DNA repair genes, which has yielded important insights into the dynamic balance between NHEJ and HR repair in cells. In addition, we have applied our system to the study of DSB repair in growth-arrested and serum-deprived cells. These experiments have revealed that mutagenic NHEJ repair is repressed under these conditions, whereas cNHEJ repair seems to be intact.

As discussed in the 'Introduction' section, several intrachromosomally based NHEJ repair assays have been described previously (20,22–26,28,66,67). Caution is warranted in comparing the results and conclusions drawn from experiments based on these assays and the one presented in the current study. Interpretation of results obtained from the assays based on two I-SceI sites could be complicated by the requirement for the induction of two synchronous DSBs instead of one, either in close proximity or at distant locations, with active repair events occurring at each site asynchronously. Clearly, synchronous cleavage with loss of the intervening sequence is not a common process in these assays, as the rates of GFP+ cells typically range between 1 and 5%. This contrasts with our findings of robust mutagenic NHEJ repair levels in multiple cell lines, as manifested by the results ranging between 10 and 60% DsRed+ cells after DSB induction. For the assays with I-SceI sites in direct orientation, it is also not known whether these sites themselves serve as regions of microhomology for specific non-canonical NHEJ repair pathways. Similarly, the NHEJ-induced inversions observed in the assay by Lopez and colleagues (23,66,67) may not be easily correlated with NHEJ repair events involving the large or small 'pop-out' fragments in the assays by the other laboratories. Regardless, these assays have yielded enormous insights into the mechanisms of NHEJ repair at intrachromosomal sites. However, we argue that additional NHEJ assays, coupled with further genetic studies, are needed to fully elucidate the spectrum of NHEJ repair pathways in mammalian cells. One particular strength of our EJ-RFP assay is that it measures the repair of a single DSB, and that it reports any type of mutagenic repair events beyond precise re-ligation. Although precise re-ligation seems to be largely cNHEJ-dependent [as shown previously and also in the present study (22,32,49)], it is likely that cNHEJ repair proteins also contribute to mutagenic NHEJ repair detected in our assay, as it has been shown that minor processing can occur at the break, depending on the type of lesion, using cNHEJ (68). We are currently unable to assess this contribution, as we and others have not been able to identify and target the proteins that mediate non-canonical NHEJ repair (12–15). One limitation of almost all NHEJ assays, including the one presented in this article, is that they do not accurately report the frequency of the precise re-ligation events at a single DSB. This is because these re-ligated sites can be re-cleaved by I-SceI multiple times, representing a cycle that can only be 'broken' by removal of the I-SceI protein, or by loss of the I-SceI recognition site via mutagenic repair of the cleavage site. The former intervention can be attempted by using ddSceGR with a shorter ligand incubation time (e.g. 1 h, as in Figure 3G), although this is limited by significantly lower DSB repair activity.

Consistent with the reports described earlier in the text, we have also observed that repression of cNHEJ shifts the balance to both HR and mutagenic NHEJ repair pathways. In contrast, our studies suggest that *CtIP* downregulation does not reduce the rates of mutagenic NHEJ repair (and in fact, we have detected increases in mutagenic NHEJ). This conflicts with previous reports that CtIP downregulation represses microhomology-dependent NHEJ (22). Interestingly, although both the Mre11 and PARP-1 proteins also seem to play a role in non-canonical NHEJ (25,26), we did not detect any reductions in mutagenic NHEJ in our assay (data not shown and Figure 4B, respectively). We also did not detect any effects on mutagenic NHEJ repair after siRNA knockdown of several key genes implicated in non-canonical NHEJ, including *LigIII* and *XRCC1*. Although these findings are surprising at *prima facie*, they are nonetheless consistent with recent reports that these proteins may not be absolutely required for non-canonical NHEJ repair (12–15). Iliakis and colleagues (56) have reported that DNA ligases may have redundant functions, which

could explain why knockdown of *LigIII* alone did not produce a phenotype. However, attempts to knockdown multiple DNA ligases (e.g. *LigI*, *Lig III* and/or *LigIV*), using a combination of short hairpin RNA (shRNA) and siRNA approaches, also did not reduce mutagenic NHEJ repair levels in our assay (data not shown). Combined knockdown of LigIV and XRCC4 substantially reduced the expression levels of LigIV beyond LigIV knockdown alone (Supplementary Figure S1G), which was also correlated with increased HR and mutagenic NHEJ repair activity (1.5-fold increases for both pathways, data not shown). Intriguingly, growth arrest and serum deprivation were the only factors that were found to reduce mutagenic NHEJ repair in the EJ-RFP assay, and these findings are consistent with previous reports (10,16–18). Further studies are necessary to determine the molecular mechanisms by which mutagenic repair is repressed under these conditions. Furthermore, it will be interesting to determine whether specific non-canonical NHEJ repair sub-pathways (e.g. mutagenic NHEJ with or without microhomology usage) are regulated by serum stimulation and/or cell cycle phase. Such studies will have important implications for tumor cell targeting with IR because of the great heterogeneity in the proliferative states of various tumors. Taken together, further studies are needed to evaluate the role(s) of each DSB repair protein in canonical and non-canonical NHEJ repair, and the broad set of repair assays for these studies will be invaluable for these inquiries.

In conclusion, our novel DSB repair assay will be an important tool to help further elucidate NHEJ sub-pathways in the future. Furthermore, the combination of EJ-RFP with DR-GFP will allow investigators to study dynamic shifts between NHEJ and HR in a manner that was not possible previously. In addition, our novel inducible I-SceI assay has many potential applications, including the study of DSB repair patterns with larger siRNA libraries, analyses of DSB induction and resolution kinetics, and also the analysis of DSB repair in specific cell cycle phases. The robust signal associated with the EJ-DR assay, and the ease of ligand-inducible cleavage with ddSceGR, makes these systems amenable for high-throughput screening studies to identify novel DSB repair inhibitors. These studies are currently ongoing in our laboratory. Furthermore, this two-tiered approach to the control of I-SceI cleavage activity likely can be applied to other proteins, including other endonucleases and zinc-fingers, as a means to better control site-specific cleavage rates in mammalian cells.

## SUPPLEMENTARY DATA

Supplementary Data are available at NAR Online: Supplementary Figures 1 and 2.

## ACKNOWLEDGEMENTS

The authors thank Petrus Hendrikx at the MSKCC flow cytometry core facility for their technical expertise and insights during the course of EJ-RFP assay development. They thank Dr Tom Misteli and Dr Eva Soutoglou for providing the SceGR plasmid and for their expertise and insights in the design of ddSceGR. R.S.B. designed and performed the research and wrote the article; A.G. designed and performed the siRNA experiments targeting key DSB repair genes, and he performed the confocal microscopy studies. M.J. provided expertise and insights during the course of initial assay development; S.N.P. designed the research and wrote the article.

## FUNDING

Brain Tumor Center MSKCC grant; Radiological Society of North America (RSNA) research resident grant (to R.S.B.). Funding for open access charge: Departmental Funds.

*Conflict of interest statement*. None declared.

## REFERENCES

1. Jackson,S.P. and Bartek,J. (2009) The DNA-damage response in human biology and disease. *Nature*, **461**, 1071–1078.
2. Bouwman,P. and Jonkers,J. (2012) The effects of deregulated DNA damage signalling on cancer chemotherapy response and resistance. *Nat. Rev. Cancer*, **12**, 587–598.
3. Polo,S.E. and Jackson,S.P. (2011) Dynamics of DNA damage response proteins at DNA breaks: a focus on protein modifications. *Genes Dev.*, **25**, 409–433.
4. Brandsma,I. and Gent,D.C. (2012) Pathway choice in DNA double strand break repair: observations of a balancing act. *Genome Integr.*, **3**, 9.
5. Lin,F.L., Sperle,K. and Sternberg,N. (1984) Model for homologous recombination during transfer of DNA into mouse L cells: role for DNA ends in the recombination process. *Mol. Cell. Biol.*, **4**, 1020–1034.
6. Mladenov,E. and Iliakis,G. (2011) Induction and repair of DNA double strand breaks: the increasing spectrum of non-homologous end joining pathways. *Mutat. Res.*, **711**, 61–72.
7. Lieber,M.R. (2010) The mechanism of double-strand DNA break repair by the nonhomologous DNA end-joining pathway. *Ann. Rev. Biochem.*, **79**, 181–211.
8. Lieber,M.R. and Wilson,T.E. (2010) SnapShot: Nonhomologous DNA end joining (NHEJ). *Cell*, **142**, 496–496 e491.
9. Corneo,B., Wendland,R.L., Deriano,L., Cui,X., Klein,I.A., Wong,S.Y., Arnal,S., Holub,A.J., Weller,G.R., Pancake,B.A. *et al.* (2007) Rag mutations reveal robust alternative end joining. *Nature*, **449**, 483–486.
10. Iliakis,G. (2009) Backup pathways of NHEJ in cells of higher eukaryotes: cell cycle dependence. *Radiother. Oncol.*, **92**, 310–315.
11. Ma,J.L., Kim,E.M., Haber,J.E. and Lee,S.E. (2003) Yeast Mre11 and Rad1 proteins define a Ku-independent mechanism to repair double-strand breaks lacking overlapping end sequences. *Mol. Cell. Biol.*, **23**, 8820–8828.
12. Simsek,D., Furda,A., Gao,Y., Artus,J., Brunet,E., Hadjantonakis,A.K., Van Houten,B., Shuman,S., McKinnon,P.J. and Jasin,M. (2011) Crucial role for DNA ligase III in mitochondria but not in Xrcc1-dependent repair. *Nature*, **471**, 245–248.
13. Han,L., Mao,W. and Yu,K. (2012) X-ray repair cross-complementing protein 1 (XRCC1) deficiency enhances class switch recombination and is permissive for alternative end joining. *Proc. Natl Acad. Sci. USA*, **109**, 4604–4608.
14. Gao,Y., Katyal,S., Lee,Y., Zhao,J., Rehg,J.E., Russell,H.R. and McKinnon,P.J. (2011) DNA ligase III is critical for mtDNA integrity but not Xrcc1-mediated nuclear DNA repair. *Nature*, **471**, 240–244.
15. Boboila,C., Oksenych,V., Gostissa,M., Wang,J.H., Zha,S., Zhang,Y., Chai,H., Lee,C.S., Jankovic,M., Saez,L.M. *et al.* (2012)

Robust chromosomal DNA repair via alternative end-joining in the absence of X-ray repair cross-complementing protein 1 (XRCC1). *Proc. Natl Acad. Sci. USA*, **109**, 2473–2478.
16. Singh,S.K., Bednar,T., Zhang,L., Wu,W., Mladenov,E. and Iliakis,G. (2012) Inhibition of B-NHEJ in plateau-phase cells is not a direct consequence of suppressed growth factor signaling. *Int. J. Radiat. Oncol. Biol. Phys.*, **84**, e237–e243.
17. Singh,S.K., Wu,W., Zhang,L., Klammer,H., Wang,M. and Iliakis,G. (2011) Widespread dependence of backup NHEJ on growth state: ramifications for the use of DNA-PK inhibitors. *Int. J. Radiat. Oncol. Biol. Phys.*, **79**, 540–548.
18. Windhofer,F., Wu,W., Wang,M., Singh,S.K., Saha,J., Rosidi,B. and Iliakis,G. (2007) Marked dependence on growth state of backup pathways of NHEJ. *Int. J. Radiat. Oncol. Biol. Phys.*, **68**, 1462–1470.
19. Pastwa,E., Somiari,R.I., Malinowski,M., Somiari,S.B. and Winters,T.A. (2009) In vitro non-homologous DNA end joining assays—the 20th anniversary. *Int. J. Biochem. Cell Biol.*, **41**, 1254–1260.
20. Gunn,A. and Stark,J.M. (2012) I-SceI-based assays to examine distinct repair outcomes of mammalian chromosomal double strand breaks. *Methods Mol. Biol.*, **920**, 379–391.
21. Pierce,A.J., Johnson,R.D., Thompson,L.H. and Jasin,M. (1999) XRCC3 promotes homology-directed repair of DNA damage in mammalian cells. *Genes Dev.*, **13**, 2633–2638.
22. Bennardo,N., Cheng,A., Huang,N. and Stark,J.M. (2008) Alternative-NHEJ is a mechanistically distinct pathway of mammalian chromosome break repair. *PLoS Genet.*, **4**, e1000110.
23. Guirouilh-Barbat,J., Rass,E., Plo,I., Bertrand,P. and Lopez,B.S. (2007) Defects in XRCC4 and KU80 differentially affect the joining of distal nonhomologous ends. *Proc. Natl Acad. Sci. USA*, **104**, 20902–20907.
24. Mansour,W.Y., Schumacher,S., Rosskopf,R., Rhein,T., Schmidt-Petersen,F., Gatzemeier,F., Haag,F., Borgmann,K., Willers,H. and Dahm-Daphi,J. (2008) Hierarchy of nonhomologous end-joining, single-strand annealing and gene conversion at site-directed DNA double-strand breaks. *Nucleic Acids Res.*, **36**, 4088–4098.
25. Xie,A., Kwok,A. and Scully,R. (2009) Role of mammalian Mre11 in classical and alternative nonhomologous end joining. *Nat. Struct. Mol. Biol.*, **16**, 814–818.
26. Mansour,W.Y., Rhein,T. and Dahm-Daphi,J. (2010) The alternative end-joining pathway for repair of DNA double-strand breaks requires PARP1 but is not dependent upon microhomologies. *Nucleic Acids Res.*, **38**, 6065–6077.
27. Wang,M., Wu,W., Rosidi,B., Zhang,L., Wang,H. and Iliakis,G. (2006) PARP-1 and Ku compete for repair of DNA double strand breaks by distinct NHEJ pathways. *Nucleic Acids Res.*, **34**, 6170–6182.
28. Schulte-Uentrop,L., El-Awady,R.A., Schliecker,L., Willers,H. and Dahm-Daphi,J. (2008) Distinct roles of XRCC4 and Ku80 in non-homologous end-joining of endonuclease- and ionizing radiation-induced DNA double-strand breaks. *Nucleic Acids Res.*, **36**, 2561–2569.
29. Aubert,M., Ryu,B.Y., Banks,L., Rawlings,D.J., Scharenberg,A.M. and Jerome,K.R. (2011) Successful targeting and disruption of an integrated reporter lentivirus using the engineered homing endonuclease Y2 I-AniI. *PloS One*, **6**, e16825.
30. Certo,M.T., Ryu,B.Y., Annis,J.E., Garibov,M., Jarjour,J., Rawlings,D.J. and Scharenberg,A.M. (2011) Tracking genome engineering outcome at individual DNA breakpoints. *Nat. Methods*, **8**, 671–676.
31. Kim,H., Um,E., Cho,S.R., Jung,C. and Kim,J.S. (2011) Surrogate reporters for enrichment of cells with nuclease-induced mutations. *Nat. Methods*, **8**, 941–943.
32. Pierce,A.J., Hu,P., Han,M., Ellis,N. and Jasin,M. (2001) Ku DNA end-binding protein modulates homologous repair of double-strand breaks in mammalian cells. *Genes Dev.*, **15**, 3237–3242.
33. Perrault,R., Wang,H., Wang,M., Rosidi,B. and Iliakis,G. (2004) Backup pathways of NHEJ are suppressed by DNA-PK. *J. Cell. Biochem.*, **92**, 781–794.
34. Soutoglou,E., Dorn,J.F., Sengupta,K., Jasin,M., Nussenzweig,A., Ried,T., Danuser,G. and Misteli,T. (2007) Positional stability of single double-strand breaks in mammalian cells. *Nat. Cell Biol.*, **9**, 675–682.
35. Richardson,C., Moynahan,M.E. and Jasin,M. (1998) Double-strand break repair by interchromosomal recombination: suppression of chromosomal translocations. *Genes Dev.*, **12**, 3831–3842.
36. Nakanishi,K., Cavallo,F., Brunet,E. and Jasin,M. (2011) Homologous recombination assay for interstrand cross-link repair. *Methods Mol. Biol.*, **745**, 283–291.
37. Lee,H.J., Kim,E. and Kim,J.S. (2010) Targeted chromosomal deletions in human cells using zinc finger nucleases. *Genome Res.*, **20**, 81–89.
38. Lok,B.H., Carley,A.C., Tchang,B. and Powell,S.N. (2012) RAD52 inactivation is synthetically lethal with deficiencies in BRCA1 and PALB2 in addition to BRCA2 through RAD51-mediated homologous recombination. *Oncogene*, Sep 10 (doi:10.1038/onc.2012.391; epub ahead of print).
39. Feng,Z., Scott,S.P., Bussen,W., Sharma,G.G., Guo,G., Pandita,T.K. and Powell,S.N. (2011) Rad52 inactivation is synthetically lethal with BRCA2 deficiency. *Proc. Natl Acad. Sci. USA*, **108**, 686–691.
40. Saenger,W., Orth,P., Kisker,C., Hillen,W. and Hinrichs,W. (2000) The tetracycline repressor-a paradigm for a biological switch. *Angew. Chem. Int. Ed. Engl.*, **39**, 2042–2052.
41. Yao,F., Svensjo,T., Winkler,T., Lu,M., Eriksson,C. and Eriksson,E. (1998) Tetracycline repressor, tetR, rather than the tetR-mammalian cell transcription factor fusion derivatives, regulates inducible gene expression in mammalian cells. *Hum. Gene Ther.*, **9**, 1939–1950.
42. Magin,S., Saha,J., Wang,M., Mladenova,V., Coym,N. and Iliakis,G. (2013) Lipofection and nucleofection of substrate plasmid can generate widely different readings of DNA end-joining efficiency in different cell lines. *DNA Repair*, **12**, 148–160.
43. Dinda,S., Sanchez,A. and Moudgil,V. (2002) Estrogen-like effects of thyroid hormone on the regulation of tumor suppressor proteins, p53 and retinoblastoma, in breast cancer cells. *Oncogene*, **21**, 761–768.
44. Aakvaag,A., Utaaker,E., Thorsen,T., Lea,O.A. and Lahooti,H. (1990) Growth control of human mammary cancer cells (MCF-7 cells) in culture: effect of estradiol and growth factors in serum-containing medium. *Cancer Res.*, **50**, 7806–7810.
45. Dang,Z.C. and Lowik,C.W. (2005) Removal of serum factors by charcoal treatment promotes adipogenesis via a MAPK-dependent pathway. *Mol. Cell. Biochem.*, **268**, 159–167.
46. Yohay,D.A., Zhang,J., Thrailkill,K.M., Arthur,J.M. and Quarles,L.D. (1994) Role of serum in the developmental expression of alkaline phosphatase in MC3T3-E1 osteoblasts. *J. Cell. Physiol.*, **158**, 467–475.
47. Banaszynski,L.A., Chen,L.C., Maynard-Smith,L.A., Ooi,A.G. and Wandless,T.J. (2006) A rapid, reversible, and tunable method to regulate protein function in living cells using synthetic small molecules. *Cell*, **126**, 995–1004.
48. Shahar,O.D., Raghu Ram,E.V., Shimshoni,E., Hareli,S., Meshorer,E. and Goldberg,M. (2012) Live imaging of induced and controlled DNA double-strand break formation reveals extremely low repair by homologous recombination in human cells. *Oncogene*, **31**, 3495–3504.
49. Stark,J.M., Pierce,A.J., Oh,J., Pastink,A. and Jasin,M. (2004) Genetic steps of mammalian homologous repair with distinct mutagenic consequences. *Mol. Cell. Biol.*, **24**, 9305–9316.
50. Convery,E., Shin,E.K., Ding,Q., Wang,W., Douglas,P., Davis,L.S., Nickoloff,J.A., Lees-Miller,S.P. and Meek,K. (2005) Inhibition of homologous recombination by variants of the catalytic subunit of the DNA-dependent protein kinase (DNA-PKcs). *Proc. Natl Acad. Sci. USA*, **102**, 1345–1350.
51. Allen,C., Halbrook,J. and Nickoloff,J.A. (2003) Interactive competition between homologous recombination and non-homologous end joining. *Mol. Cancer Res.*, **1**, 913–920.
52. Delacote,F., Han,M., Stamato,T.D., Jasin,M. and Lopez,B.S. (2002) An xrcc4 defect or Wortmannin stimulates homologous recombination specifically induced by double-strand breaks in mammalian cells. *Nucleic Acid Res.*, **30**, 3454–3463.
53. Clikeman,J.A., Khalsa,G.J., Barton,S.L. and Nickoloff,J.A. (2001) Homologous recombinational repair of double-strand breaks

in yeast is enhanced by MAT heterozygosity through yKU-dependent and -independent mechanisms. *Genetics*, **157**, 579–589.
54. Fukushima,T., Takata,M., Morrison,C., Araki,R., Fujimori,A., Abe,M., Tatsumi,K., Jasin,M., Dhar,P.K., Sonoda,E. *et al.* (2001) Genetic analysis of the DNA-dependent protein kinase reveals an inhibitory role of Ku in late S-G2 phase DNA double-strand break repair. *J. Biol. Chem.*, **276**, 44413–44418.
55. Fattah,F., Lee,E.H., Weisensel,N., Wang,Y., Lichter,N. and Hendrickson,E.A. (2010) Ku regulates the non-homologous end joining pathway choice of DNA double-strand break repair in human somatic cells. *PLoS Genet.*, **6**, e1000855.
56. Arakawa,H., Bednar,T., Wang,M., Paul,K., Mladenov,E., Bencsik-Theilen,A.A. and Iliakis,G. (2012) Functional redundancy between DNA ligases I and III in DNA replication in vertebrate cells. *Nucleic Acids Res.*, **40**, 2599–2610.
57. Sartori,A.A., Lukas,C., Coates,J., Mistrik,M., Fu,S., Bartek,J., Baer,R., Lukas,J. and Jackson,S.P. (2007) Human CtIP promotes DNA end resection. *Nature*, **450**, 509–514.
58. Wang,H., Shao,Z., Shi,L.Z., Hwang,P.Y., Truong,L.N., Berns,M.W., Chen,D.J. and Wu,X. (2012) CtIP protein dimerization is critical for its recruitment to chromosomal DNA double-stranded breaks. *J. Biol. Chem.*, **287**, 21471–21480.
59. Quennet,V., Beucher,A., Barton,O., Takeda,S. and Lobrich,M. (2011) CtIP and MRN promote non-homologous end-joining of etoposide-induced DNA double-strand breaks in G1. *Nucleic Acids Res.*, **39**, 2144–2152.
60. Takata,M., Sasaki,M.S., Sonoda,E., Morrison,C., Hashimoto,M., Utsumi,H., Yamaguchi-Iwai,Y., Shinohara,A. and Takeda,S. (1998) Homologous recombination and non-homologous end-joining pathways of DNA double-strand break repair have overlapping roles in the maintenance of chromosomal integrity in vertebrate cells. *EMBO J.*, **17**, 5497–5508.
61. Hsu,S.C., Qi,M. and DeFranco,D.B. (1992) Cell cycle regulation of glucocorticoid receptor function. *EMBO J.*, **11**, 3457–3468.
62. Rogatsky,I., Trowbridge,J.M. and Garabedian,M.J. (1997) Glucocorticoid receptor-mediated cell cycle arrest is achieved through distinct cell-specific transcriptional regulatory mechanisms. *Mol. Cell. Biol.*, **17**, 3181–3193.
63. Carriere,A., Cargnello,M., Julien,L.A., Gao,H., Bonneil,E., Thibault,P. and Roux,P.P. (2008) Oncogenic MAPK signaling stimulates mTORC1 activity by promoting RSK-mediated raptor phosphorylation. *Curr. Biol.*, **18**, 1269–1277.
64. Giehl,K., Skripczynski,B., Mansard,A., Menke,A. and Gierschik,P. (2000) Growth factor-dependent activation of the Ras-Raf-MEK-MAPK pathway in the human pancreatic carcinoma cell line PANC-1 carrying activated K-ras: implications for cell proliferation and cell migration. *Oncogene*, **19**, 2930–2942.
65. Dobbs,T.A., Tainer,J.A. and Lees-Miller,S.P. (2010) A structural model for regulation of NHEJ by DNA-PKcs autophosphorylation. *DNA Repair*, **9**, 1307–1314.
66. Guirouilh-Barbat,J., Huck,S., Bertrand,P., Pirzio,L., Desmaze,C., Sabatier,L. and Lopez,B.S. (2004) Impact of the KU80 pathway on NHEJ-induced genome rearrangements in mammalian cells. *Mol. Cell*, **14**, 611–623.
67. Rass,E., Grabarz,A., Plo,I., Gautier,J., Bertrand,P. and Lopez,B.S. (2009) Role of Mre11 in chromosomal nonhomologous end joining in mammalian cells. *Nat. Struct. Mol. Biol.*, **16**, 819–824.
68. Hefferin,M.L. and Tomkinson,A.E. (2005) Mechanism of DNA double-strand break repair by non-homologous end joining. *DNA Repair*, **4**, 639–648.